NÖHÜ Müh. Bilim. Derg. / NOHU J. Eng. Sci., 2025; 14(3), 1082-1087

Niğde Ömer Halisdemir Üniversitesi Mühendislik Bilimleri Dergisi
Niğde Ömer Halisdemir University Journal of Engineering Sciences

Araştırma makalesi / Research article

www.dergipark.org.tr/tr/pub/ngumuh / www.dergipark.org.tr/en/pub/ngumuh

Enhanced hydrogen storage via NaH and GO composites: Structural, morphological and spectroscopic insights

NaH ve GO kompozitleri ile geliştirilmiş hidrojen depolama: Yapısal, morfolojik ve spektroskopik incelemeler

Ali Altuntepe[1,*]

[1] *Optical Excellence Application and Research Center, Sivas University of Science and Technonogy, Sivas, 58000, Türkiye*

Abstract

In this work, a novel composite material composed of NaH and GO was prepared and investigated for hydrogen storage. The composite was prepared using ball milling techniques and was also characterized by Raman spectroscopy, XRD, BET measurements, and SEM. Raman spectroscopy established hydrogenation induced the formation of large defects in the GO matrix and shifts in phonon modes of NaH vibrational modes, establishing structural changes through hydrogen interaction. XRD findings indicated lattice contraction and decrease in crystallite size upon hydrogen absorption, and secondary phases such as NaOH and NaO_2H_3 were also present due to the sensitivity of NaH to environmental oxygen and humidity. BET analysis revealed a surface area of 9.42 m^2/g with an average pore diameter of ≤68.79 nm, and SEM images confirmed a well-dispersed, fractured morphology for hydrogen uptake. Hydrogen storage capacities at 5, 10, and 15 bar showed pressure-dependent behavior, and the composite was observed to achieve a maximum capacity of 1.9 wt% at 15 bar. The interaction between GO and NaH enhances structural stability, surface accessibility, and defect density, making the NaH+GO composite a promising candidate for high-efficiency solid-state hydrogen storage applications.

Anahtar kelimeler: NaH, GO, Hydrogen storage, Ball milling

Öz

Bu çalışmada, NaH ve GO'dan oluşan yeni bir kompozit malzeme hazırlanmış ve hidrojen depolama amacıyla incelenmiştir. Kompozit, bilyalı öğütme (ball milling) yöntemiyle sentezlenmiş ve Raman spektroskopisi, XRD, BET yüzey alanı ölçümleri ve SEM ile karakterize edilmiştir. Raman spektroskopisi, hidrojenleme işleminin GO matrisi içerisinde büyük yapısal kusurlar oluşturduğunu ve NaH'nin titreşim modlarında fonon kaymalarına neden olduğunu, dolayısıyla hidrojen etkileşimiyle yapısal değişimlerin meydana geldiğini ortaya koymuştur. XRD sonuçları, hidrojen absorpsiyonu sonrası kristal örgüsünde daralma ve kristalit boyutunda azalma olduğunu göstermiştir. Ayrıca, NaH'nin çevresel oksijen ve nem hassasiyetinden kaynaklı olarak NaOH ve NaO_2H_3 gibi ikincil fazlara da rastlanmıştır. BET analizine göre, kompozitin yüzey alanı 9.42 m^2/g ve ortalama gözenek çapı ≤68.79 nm olarak belirlenmiştir. SEM görüntüleri, hidrojen alımı için uygun, iyi dağılmış ve kırık morfolojiyi doğrulamıştır. 5, 10 ve 15 bar basınçlarda yapılan hidrojen depolama testlerinde, basınca bağlı bir davranış gözlemlenmiş ve kompozitin 15 bar'da maksimum %1.9 ağırlıkça hidrojen depolama kapasitesine ulaştığı belirlenmiştir. GO ve NaH arasındaki sinerjik etkileşim, yapısal kararlılığı, yüzey erişilebilirliğini ve kusur yoğunluğunu artırarak, NaH+GO kompozitini yüksek verimli katı hâl hidrojen depolama uygulamaları için umut vadeden bir malzeme haline getirmiştir.

Keywords: NaH, GO, Hidrojen depolama, Bilyalı değirmen

1 Introduction

Hydrogen, the lightest and simplest element in the universe, contains only a proton and an electron [1]. Hydrogen is not found free in nature but is ubiquitous as compounds like water, a condition of life, and hydrocarbons, basic fuels of the contemporary world. Hydrogen, due to its extremely high energy density of nearly three times that of petroleum, possesses a highly immense ability to fulfill future energy requirements. Nevertheless, a number of issues are still present in achieving an economy based on hydrogen, the storage of hydrogen being one of the greatest hurdles. Storage in high-pressure containers [2] and cryogenic storage [3], although technologically possible, are not well suited for everyday vehicular use because of their low energy densities and attendant safety issues. Consequently, a lot of research has gone into creating solid-state materials that can reversibly store hydrogen safely and efficiently.

NaH possesses a crystalline structure composed of sodium ions (Na^+) and hydride ions (H^-). In hydrogen storage applications, sodium hydride is notable for its ability to absorb and release hydrogen gas. NaH is widely used in chemical synthesis as a Brønsted base and readily reacts with various Brønsted acids. However, it rarely behaves as if it delivers the hydride to polar π electrophiles in a direct

* Sorumlu yazar / Corresponding author, e-posta / e-mail: altuntepeali@gmail.com (A. Altuntepe)
Geliş / Received: 24.04.2025 Kabul / Accepted: 16.06.2025 Yayımlanma / Published: 15.07.2025
doi: 10.28948/ngumuh.1681889

manner. This unique behavior makes NaH an intriguing compound among metal hydrides [4]. The main challenges in the commercialization of NaH as a hydrogen storage material are its high reactivity and hygroscopic nature. NaH is also a strong base and can readily react with various substances. Nevertheless, ongoing research is focused on developing new methods for the safe handling and storage of NaH to overcome these limitations. Sodium hydride-based hydrogen storage systems have diverse applications in the field of energy storage and transport. In particular, they hold promise for use in vehicles and renewable energy systems, where they can be integrated with hydrogen fuel cells to help address the challenges of energy storage and distribution.

Hydrogen storage as chemical bonding or surface adsorption on carbonaceous materials is more safe, as it typically requires controlled energy input to evolve the stored hydrogen [5]. This intrinsic stability has stimulated keen interest in the research and development of emerging storage technologies. Among the many directions that have been explored, metal hydrides, chemical hydrides, and high-performance carbon nanostructures have been at the forefront [6]. In particular, these kinds of materials like activated carbon, carbon nanotubes, and carbon nanofibers have been intensively investigated due to their high surface areas and controllable porosity. Although earlier research has reported enormous hydrogen adsorption in these carbon materials, experimental findings have resulted in enormous discrepancies. Storage capacities vary by several orders of magnitude between different experiments, and the very high ones reported in a few papers have resisted replication in highly controlled laboratory conditions, their validity and utility questionable.

In the case of defected graphene, metal atoms tend to remain closer to the substrate and exhibit stronger binding energies compared to those on pristine graphene. This behavior is primarily attributed to the presence of single-vacancy defects, which play a role in mitigating the aggregation of transition metal atoms. Such defects enable the distribution of individual metal atoms across the graphene surface, potentially creating multiple isolated catalytic or adsorption sites across a wide nanosheet [7-8]. Conversely, even on defect-free graphene, transition metals can enhance hydrogen adsorption due to electronic effects such as charge transfer and resonance interactions induced by the metal atoms. These interactions lead to an increased polarization of hydrogen bonds, potentially resulting in dipole-dipole attractions. Overall, non-pristine graphene whether through structural defects or surface functionalization exhibits stronger hydrogen interactions [9, 10]. However, the suppression of metal clustering through defect engineering remains limited, as clustering tendencies often re-emerge despite defect-induced stabilization.

Carbon additives such as CNTs or carbon blacks were shown to improve the hydrogen sorption kinetics of complex hydrides such as $NaAlH_4$ or MgH_2 by nanoconfinement or catalytic processes [2], our composite is the first one to demonstrate that even simple ball-milling of NaH with GO (graphene oxide) can create extensive defects, shifts in the phonons, and enhanced pressure-sensitive storage capacity (up to 1.9 wt% at 15 bar). Particularly, I_D/I_G ratio alteration from 0.89 to 1.41 and reduction of crystallite size (from 3.64 to 3.34 nm) demonstrate the formation of defect sites and microstrain in GO-NaH matrix processes consistent with hydrogen-induced lattice distortion and interfacial polarization accounted for by Adelhelm et al [7]. Also, Na's intercalation capability in defective carbon structures, already observed in NaH/C compounds, will likely be responsible for the described synergistic uptake behavior [7]. Different from previous work where carbon served as a dispersant or a scaffold at best, this work represents combined efforts from defect engineering, phonon mode softening, and microstructural stabilization—the three inextricably linked facets required in the design of functional solid-state hydrogen storage systems.

In this study, a GO+NaH (1:1) composite material is prepared to examine its prospect in hydrogen storage applications. GO has garnered vast research attention due to its vast surface area, reversible chemistry, and rich oxygen content of oxygenated functional groups that facilitate metal hydride particles' dispersion and anchoring with high efficiency. In contrast, NaH is known for having high hydrogen content and high reactivity but limited practical application due to safety issues and its propensity for aggregation. Incorporating NaH into GO is suggested as a means to transcend these disadvantages based on synergistic interaction between the two substances. This strategy targets the improvement of the stability, dispersibility, and hydrogen adsorption performance of NaH, which might have implications for the more efficient hydrogen storage solid-state systems.

2 Material and method

In this study, the Hummers method was employed as the basis for the synthesis of GO. Initially, a specified amount of sulfuric acid (H_2SO_4) and 0.2 g of potassium permanganate ($KMnO_4$) were added into a 100 mL beaker and stirred for 30 minutes. Subsequently, graphite powder was added to the mixture, and stirring continued. The process proceeded with the addition of distilled water, at which point the resulting mixture turned a dark brown color. During synthesis, the temperature of the mixture was critical and was maintained at approximately 4°C using an ice bath. In the next step, hydrogen peroxide (H_2O_2) was added, and the color of the mixture turned light yellow. The resulting mixture was filtered, dried at room temperature, and the dried product was re-dispersed in distilled water. This solution was subjected to sonication for several hours to exfoliate the graphite oxide layers, thereby yielding GO. After filtration, the product was washed sequentially with distilled water and methanol and then dried at 70°C to obtain GO.

To prepare NaH and GO composites, ball milling was performed. Steel balls of 6.4 mm and 3.2 mm diameter were used for the ball milling process to create the desired compositions. The rotation speed of the ball mill was set to 500 rpm to ensure effective friction and breakdown between the powder and the balls. The milling chamber and the balls were maintained at 20°C during grinding. Ball milling was performed for a total of 30 min in order to achieve good

dispersion and particle size reduction of NaH. The treatment was carried out in an argon (Ar) controlled environment to prevent unwanted oxidation or hydrolysis due to the high reactivity and hygroscopicity of NaH.

A finless reactor (100 mL), made of St. 42 steel, was used as the hydrogen storage reactor. To evacuate moisture and air from the reactor, a vacuum of up to 10^{-2} Torr was applied using a vacuum pump. Additionally, a thermal treatment (annealing at 200°C for 15 minutes) was conducted with a heating plate to remove any remaining moisture and organic contaminants inside the reactor. Argon gas was used to inert the inside of the reactor to ensure complete removal of moisture. The hydrogen used for storage had a purity of 99.9999%. For the hydrogen storage process, the powdered samples were exposed to 5, 10, and 15 bar H_2 pressure for 30 minutes. This allowed for the diffusion of H_2 into the materials and completion of the hydrogen storage process. To enhance the hydrogen activation rate, this procedure will be repeated four times. The pressure values were determined based on literature and the gas output capacity of the current regulator [11, 12]. Initially, all experimental parameters were carried out at room temperature. Hydrogen storage capacity measurements were performed using a custom-built volumetric setup equipped with an Alicat Scientific mass flow controller (MFC, model: Alicat MC Series) to precisely regulate and monitor hydrogen gas flow during pressurization. The system also included a calibrated pressure transducer (range: 0–20 bar, resolution: ±0.01 bar) and a stainless steel reactor chamber designed to withstand hydrogen environments. Before each measurement, the chamber was evacuated to 10^{-2} Torr using a rotary vacuum pump and purged multiple times with 99.999% pure argon to ensure an inert atmosphere. Flow regulation by the Alicat MFC ensured consistent hydrogen delivery, while the reactor temperature and pressure were continuously monitored. All measurements were repeated in triplicate for statistical validation and reproducibility. The structural, morphological, and surface characteristics of the NaH+GO composites were examined using Raman spectroscopy, X-ray diffraction (XRD), Brunauer–Emmett–Teller (BET) analysis, and scanning electron microscopy (SEM). Raman spectroscopy was employed to identify structural defects, phonon mode shifts, and hydrogen-induced changes in the GO matrix and NaH structure.

3 Result and discussion

Raman spectroscopy was used to investigate the structural change and hydrogen interaction behavior of the as-prepared NaH+GO and hydrogenated NaH+GO (H-NaH+GO) composites. The corresponding Raman spectra are presented in Figure 1. Two regions were investigated: the low-frequency region for the vibration modes of NaH and the higher-frequency region for the graphene oxide carbon skeleton. Two intense bands at ~1340 cm^{-1} and ~1600 cm^{-1} in both spectra are due to the D-band and G-band of graphene oxide, respectively [13, 14]. The D-band represents structural disorder and defects in the sp^2 carbon lattice, while the G-band is attributed to the E_{2g} vibrational mode of sp^2-bonded carbon atoms. For NaH+GO composite, D and G bands are observed at approximately 1350 cm^{-1} and 1620 cm^{-1} in Figure 1 with an intensity ratio (I_D/I_G) of ~0.89, indicating a moderate disorder in the GO structure. There are significant changes in the spectrum of H-NaH+GO upon hydrogen absorption. The D and G band positions shift to 1329 cm^{-1} and 1578 cm^{-1}, respectively. More importantly, the I_D/I_G ratio increases to ~1.41, revealing a considerable defect density enhancement of the GO lattice. This is a result of the disruption of the carbon network by hydrogen incorporation, which creates more sp^3 hybridized regions and localized distortions. The broadening of the G-band in the H-NaH+GO spectrum also supports the occurrence of hydrogenation-induced structural deformation within the carbon matrix. Two Raman bands from NaH vibrational modes at 250 cm^{-1} and 1100 cm^{-1} are observed for the NaH+GO composite in the low-frequency region [15]. With hydrogen absorption, these peaks are marginally shifted to 258 cm^{-1} and 1115 cm^{-1}, respectively. These redshifts are consistent with literature-reported phonon softening effects caused by hydrogen absorption, which disturb the local vibrational environment of the sodium hydride lattice. It is concluded that the incorporation of hydrogen into the structure of NaH influences diffusion paths of Na^+ ions believed to be along major crystallographic directions ([100], [010], and [001]) and induces minor structural reorganization on the atomic scale [16]. These findings collectively demonstrate that both the GO matrix and the NaH component are significantly modified through exposure to hydrogen.

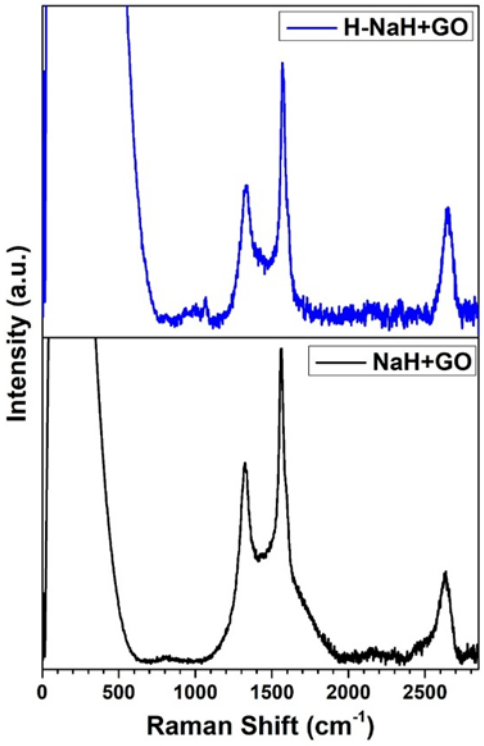

Figure 1. Raman spectra of NaH+GO (bottom, black) and H-NaH+GO (top, blue) composites

The GO framework is made more defective, with potential enhancement of hydrogen adsorption capacity, and the NaH lattice is modified at the phonon level, consistent with the incorporation of hydrogen. These synergistic effects show that the NaH+GO composite system is viable for enhanced hydrogen storage applications, in which both adsorption and defect-enhanced desorption mechanisms can be engaged. The XRD patterns of the synthesized NaH+GO and H-NaH+GO composites are presented in Figure 2. Distinct peaks in both samples confirm the presence of crystalline phases, including NaH, NaOH, NaO_2H_3, and carbon, as well as the structural changes occurring after hydrogenation. In the NaH+GO composite (black curve), the main diffraction peaks corresponding to NaH are observed at $2\theta = 31.8°$, 36.9°, 78.6°, respectively (JCPDS 98-002-8557). Additional reflections at 15.78°, 30.37°, 36.23°, 38.27°, 43.4°, 44.6°, 48.2° are assigned to NaOH phases (JCPDS 98-003-8557), while peaks at 14.87°, 33.5°, and 39.75° are indexed to NaO_2H_3 phases (JCPDS 98-002-8557). These compounds are known by products due to the high reactivity of NaH with ambient moisture and oxygen.

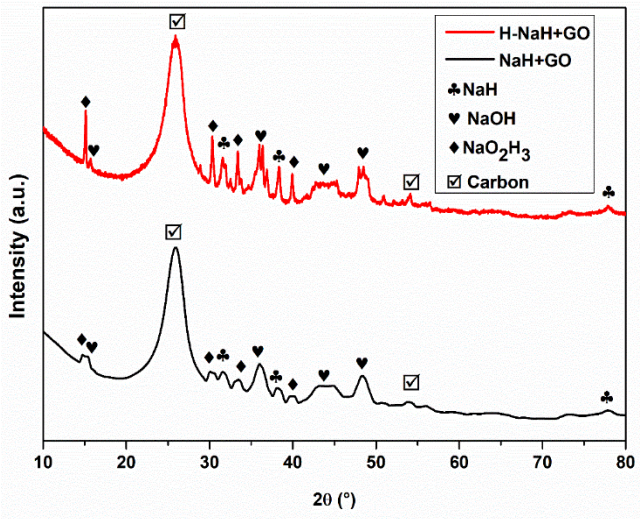

Figure 2. XRD patterns of NaH+GO (black) and H-NaH+GO (red) composites

The presence of characteristic carbon peaks ($2\theta = 10.43°$) in both composites confirms the structural contribution of GO. After hydrogenation, the H-NaH+GO sample (red curve) exhibits similar phase peaks, yet notable shifts in diffraction peak positions are observed. For instance, the NaH (111) peak shifts from 31.8° to 31.90°, indicating a decrease in interplanar spacing (d-spacing) from 3.5 Å to 3.3 Å, attributed to hydrogen incorporation into the NaH lattice. Additionally, peak broadening and intensity changes are evident, reflecting increased lattice disorder and reduced crystallite size from 3.64 nm in NaH+GO to 3.34 nm in H-NaH+GO. These changes suggest that hydrogenation induces structural strain, point defects, and possible changes in grain boundaries, all of which influence ion diffusion behavior [17]. The formation of structural defects is particularly important in hydrogen storage applications. These defects can act as diffusion pathways or trap sites for hydrogen, thereby influencing both hydrogen absorption and desorption kinetics [18]. The observed modifications in the crystal lattice, including peak shifts and broadening, underscore the importance of hydrogen-induced lattice dynamics in enhancing storage performance.

The surface area and porosity characteristics of the NaH+GO composite were investigated using the BET technique. As shown in Figure 3, the nitrogen adsorption–desorption isotherms and pore size distribution curves reveal critical insights into the structural features of the synthesized material. The specific surface area of the NaH+GO sample was found to be $9.42 m^2/g$, with a corresponding average pore size of approximately ≤68.79 nm. These results suggest that the incorporation of GO and the mechanical ball milling of NaH particles effectively increased the surface area compared to commercial NaH powders, as reported in previous studies [19]. Moreover, the presence of GO likely contributes to additional surface development due to its high surface-to-volume ratio and layered structure. This increase in surface area and pore accessibility is highly beneficial for hydrogen storage applications, as it promotes faster hydrogen diffusion and provides more sites for adsorption or chemical bonding. These textural modifications play a crucial role in improving the kinetic behavior and reversible storage capacity of the NaH+GO composite.

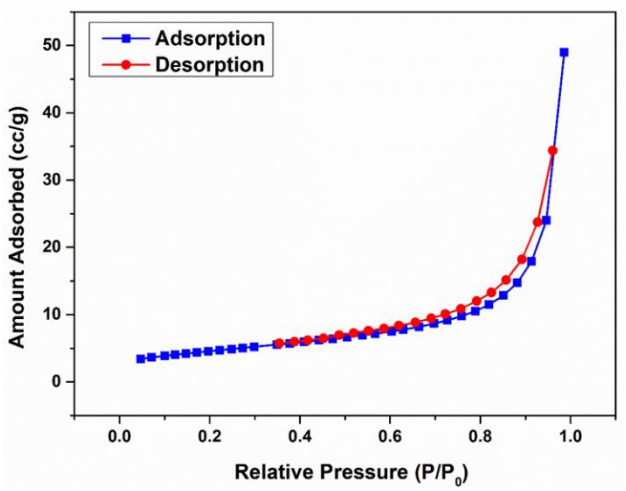

Figure 3. BET analysis of NaH+GO composite

The surface and particle morphology of the composite NaH+GO was examined with a SEM at different magnifications, respectively, and shown in Figure 4 (a-b). The micrographs display important information regarding the effect of ball milling and GO addition on the structural features of the composite. At 10,000× magnification, the NaH+GO particles have irregular block-like morphologies with fragmented and rough surfaces. The texture represents particle deformation and fracture, as expected due to the mechanical stress undergone during milling. The presence of nanoscale surface features suggests a high concentration of active surface sites that will be helpful for hydrogen adsorption and chemical reactivity. The lower magnification view (1, 000×) is a more even particle distribution over a larger area. The particles appear to be well dispersed with

reduced agglomeration, which is essential for even hydrogen diffusion and enhanced kinetics. There are also some rod-shaped and bigger clusters, which could be residual graphite or agglomerated NaH domains.

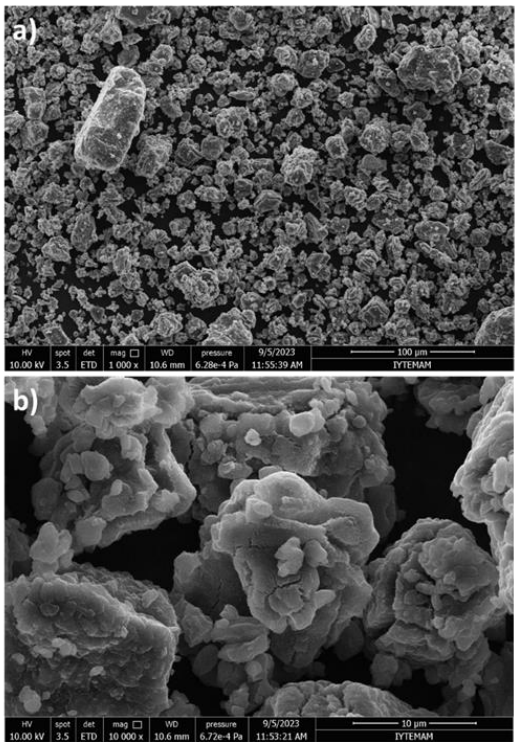

Figure 4. SEM images of NaH+GO composite at (a) 1000× and (b) 10000× magnifications

The capacity for hydrogen storage in NaH+GO composite was measured at pressures of 5, 10, and 15 bar, and values are given in Figure 5. The enhancement of hydrogen uptake is consistent with pressure, thus establishing the pressure-dependent behavior of the absorption process. For a pressure of 5 bar, hydrogen storage capacity was 1.6 wt%. Raising the pressure to 10 bar raised the storage capacity to 1.8 wt%, indicating additional hydrogen adsorption and, most likely, partial hydride formation. A further increase of the pressure to 15 bar resulted in a slight but definite rise, with a storage capacity of 1.9 wt%. The slight rise suggests that the material is very close to saturation at pressure levels above 15 bar with the experimental conditions used. This observed trend is owing to the synergy between GO that provides additional surface area, defects sites, and prevents agglomeration of particles and NaH, high-affinity hydrogen material. Increased diffusion of hydrogen is enhanced, as well as improved accessibilities to active sites, owing to synergy. Also reflecting in its modest value increase from 10 to 15 bar, a sign is presented that the easily accessible majority sites are saturated by 10 bar and extra increase in pressure simply improves marginally the hydrogen uptake. These results indicate that the NaH+GO composite exhibits promising hydrogen storage capacity even at relatively low to moderate pressures and is a potential candidate for practical solid-state hydrogen storage systems.

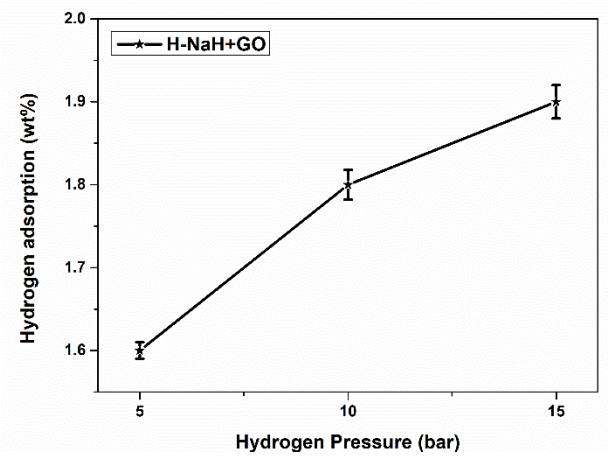

Figure 5. Hydrogen storage capacities of NaH+GO composite at different pressures

4 Conclusion

In this work, the hydrogen storage characteristic of NaH+GO composite material was investigated by structural and spectroscopic analyses prior to and after hydrogenation. The inert atmosphere-synthesized ball-milled composite with 1:1 weight ratio exhibited superior structural change upon hydrogen exposure. Raman spectroscopy showed an increase in I_D/I_G ratio, an indicator of defect formation, while XRD analysis showed changes in the peaks and reduction in crystallite size, which are evidences of lattice strain and structural distortion. The highest hydrogen storage capacity was found to be 1.9 wt% at 15 bar, which is evidence of the efficiency of the GO-supported NaH system. The results show GO inhibits not just particle agglomeration but also surface activation and the formation of defects with enhanced hydrogen uptake. These observations signal the potential of NaH+GO composites as solid-state hydrogen storage materials and set the stage for the optimization of composition and process parameters.

Similarity (iThenticate): 4%

References

[1] M. R. Usman, Hydrogen storage methods: Review and current status. Renewable and Sustainable Energy Reviews, 167, 112743, 2022. https://doi.org/10.1016/j.rs er.2022.112743.

[2] M. Zhang, H. Lv, H. Kang, W. Zhou, C. Zhang, A literature review of failure prediction and analysis methods for hydrogen storage tanks. International Journal of Hydrogen Energy, 44, 25777–25799, 2019. https://doi.org/10.1016/j.ijhydene.2019.08.028.

[3] S. Bosu, N. Rajamohan, Recent advancements in hydrogen storage—Comparative review on methods, operating conditions and challenges. International Journal of Hydrogen Energy, 52, 352–370, 2024. https://doi.org/10.1016/j.ijhydene.2023.10.005.

[4] P. C. Too, G. H. Chan, Y. L. Tnay, H. Hirao, S. Chiba, Hydride reduction by NaH–iodide composite. Angewandte Chemie International Edition, 55,3719–3723, 2016. https://doi.org/10.1002/anie.201600305.

[5] Y. Yürüm, A. Taralp, T. N. Veziroğlu, Storage of hydrogen in nanostructured carbon materials. International Journal of Hydrogen Energy, 34, 3784–3798, 2009. https://doi.org/10.10 16/j.ijhydene. 2009.03.001.

[6] Y. Liu, W. Zhang, X. Zhang, L. Yang, Nanostructured light metal hydride: Fabrication strategies and hydrogen storage performance. Renewable and Sustainable Energy Reviews, 184, 113560, 2023. https://doi.org/10.1016/j.rser.2023.113560.

[7] P. Adelhelm, The impact of carbon materials on the hydrogen storage properties of light metal hydrides. Journal of Materials Chemistry, 21, 2417–2427, 2011. https://doi.org/10.1039/C0JM02593C.

[8] H. G. Shiraz, O. Tavakoli, Investigation of graphene-based systems for hydrogen storage. Renewable and Sustainable Energy Reviews, 74, 104–109, 2017. https://doi.org/10.1016/j.rser.2017.02.052.

[9] D. S. L. Abergel, V. Apalkov, J. Berashevich, K. Ziegler, Properties of graphene: A theoretical perspective. Advances in Physics, 59, 2010. https://doi.org/10.1080/00018732.2010.487978.

[10] Z. Ao, S. Dou, Z. Xu, Hydrogen storage in porous graphene with Al decoration. International Journal of Hydrogen Energy, 39, 16244–16251, 2014. https://doi.org/10.1016/j.ijhydene.2014.08.013.

[11] M. Kayfeci, F. Bedir, Metal Hidrür Esaslı Hidrojen Depolama Reaktör Dizaynı ve Hidrojen Şarj Basıncı Etkisinin Deneysel Olarak İncelenmesi. Isı Bilimi ve Tekniği Dergisi, 34, 83–91, 2014. https://dergipark.org.tr/tr/pub/isibted/issue/33969/375 975.

[12] C. H. Chen, T. Y. Chung, C. C. Shen, M. S. Yu, C. S. Tsao, G. N. Shi, Hydrogen storage performance in palladium-doped graphene/carbon composites. International Journal of Hydrogen Energy, 38, 2013. https://doi.org/10.1016/j.ijhydene.2013.01.070.

[13] R. Krishna, E. Titus, O. Okhay, J. C. Gil, J. Ventura, E. V. Ramana, Rapid electrochemical synthesis of hydrogenated graphene oxide using Ni nanoparticles. International Journal of Electrochemical Science, 9, 4054–4069, 2014. https://doi.org/10.1016/S1452-3981(23)08073-2.

[14] R. Zan, A. Altuntepe, Nitrogen doping of graphene by CVD. Journal of Molecular Structure, 1199, 127026, 2020. https://doi.org/10.1016/j.molstruc.2019.127026.

[15] T. Marqueño, I. Osmond, P. Dalladay-Simpson, A. Hermann, R. T. Howie, High pressure study of sodium trihydride. Frontiers in Chemistry, 2024. https://doi.org/10.3389/fchem.2023.1306495.

[16] T. Famprikis, H. Bouyanfif, P. Canepa, M. Zbiri, J. A. Dawson, E. Suard, Insights into the rich polymorphism of the Na^+ ion conductor Na_3PS_4 from the perspective of variable-temperature diffraction and spectroscopy. Chemistry of Materials, 33, 5652–5667, 2021. https://doi.org/10.1021/acs.chemmater.1c01113.

[17] A. Altuntepe, S. Çelik, R. Zan, Optimizing hydrogen storage and fuel cell performance using carbon-based materials: Insights into pressure and surface area effects. Hydrogen, 6, 22, 2025. https://doi.org/10.3390/hydrogen6020022.

[18] S. Singh, S. W. H. Eijt, Hydrogen vacancies facilitate hydrogen transport kinetics in sodium hydride nanocrystallites. Physical Review B, 78, 224110, 2008. https://doi.org/10.1103/PhysRevB.78.224110.

[19] Y. Fan, W. Li, Y. Zou, S. Liao, J. Xu, Chemical reactivity and thermal stability of nanometric alkali metal hydrides. Journal of Nanoscience and Nanotechnology, 8, 935–942, 2006. https://doi. org/10.1166/jnn.2008.033.